



Article

Spectral Reflectance Indices as a High Throughput Selection Tool in a Sesame Breeding Scheme

Christos Petsoulas ¹, Eleftherios Evangelou ¹, Alexandros Tsitouras ¹, Vassilis Aschonitis ² ,
Anastasia Kargiotidou ¹ , Ebrahim Khah ³, Ourania I. Pavli ³ and Dimitrios N. Vlachostergios ^{1,*}

¹ Institute of Industrial and Forage Crops, Hellenic Agricultural Organization-Dimitra, 41335 Larissa, Greece; petsoulaschristos@elgo.gr (C.P.); evangelou@elgo.gr (E.E.); tsitalex@elgo.gr (A.T.); nastia_kar@hotmail.com (A.K.)

² Soil and Water Resources Institute, Hellenic Agricultural Organization-Dimitra, 57001 Thessaloniki, Greece; v.aschonitis@swri.gr

³ Department of Agriculture Crop Production and Rural Environment, University of Thessaly, 38446 Volos, Greece; ekhah@uth.gr (E.K.); ouraniapavli@uth.gr (O.I.P.)

* Correspondence: vlachostergios@elgo.gr

Abstract: On-farm genotype screening is at the core of every breeding scheme, but it comes with a high cost and often high degree of uncertainty. Phenomics is a new approach by plant breeders, who use optical sensors for accurate germplasm phenotyping, selection and enhancement of the genetic gain. The objectives of this study were to: (1) develop a high-throughput phenotyping workflow to estimate the Normalized Difference Vegetation Index (NDVI) and the Normalized Difference Red Edge index (NDRE) at the plot-level through an active crop canopy sensor; (2) test the ability of spectral reflectance indices (SRIs) to distinguish between sesame genotypes throughout the crop growth period; and (3) identify specific stages in the sesame growth cycle that contribute to phenotyping accuracy and functionality and evaluate the efficiency of SRIs as a selection tool. A diversity panel of 24 sesame genotypes was grown at normal and late planting dates in 2020 and 2021. To determine the SRIs the Crop Circle ACS-430 active crop canopy sensor was used from the beginning of the sesame reproductive stage to the end of the ripening stage. NDVI and NDRE reached about the same high accuracy in genotype phenotyping, even under dense biomass conditions where “saturation” problems were expected. NDVI produced higher broad-sense heritability (max 0.928) and NDRE higher phenotypic and genotypic correlation with the yield (max 0.593 and 0.748, respectively). NDRE had the highest relative efficiency (61%) as an indirect selection index to yield direct selection. Both SRIs had optimal results when the monitoring took place at the end of the reproductive stage and the beginning of the ripening stage. Thus, an active canopy sensor as this study demonstrated can assist breeders to differentiate and classify sesame genotypes.

Keywords: sesame; phenotyping; spectral reflectance; NDVI; NDRE; indirect selection



Citation: Petsoulas, C.; Evangelou, E.; Tsitouras, A.; Aschonitis, V.; Kargiotidou, A.; Khah, E.; Pavli, O.I.; Vlachostergios, D.N. Spectral Reflectance Indices as a High Throughput Selection Tool in a Sesame Breeding Scheme. *Remote Sens.* **2022**, *14*, 2629. <https://doi.org/10.3390/rs14112629>

Academic Editor: Shawn C. Kefauver

Received: 27 March 2022

Accepted: 24 May 2022

Published: 31 May 2022

Publisher's Note: MDPI stays neutral with regard to jurisdictional claims in published maps and institutional affiliations.



Copyright: © 2022 by the authors. Licensee MDPI, Basel, Switzerland. This article is an open access article distributed under the terms and conditions of the Creative Commons Attribution (CC BY) license (<https://creativecommons.org/licenses/by/4.0/>).

1. Introduction

Modern agriculture and food production systems have to withstand escalating pressure from climate change, land and water availability, and more recently, a pandemic. Sesame (*Sesamum indicum* L., $2n = 2x = 26$), one of the oldest oil crops, was domesticated about 3500 years ago from *Sesamum indicum* subsp. *Malabaricum* in the Indian sub-continent and has been cultivated since then in subtropical and temperate regions around the world [1–3]. In 2019, mainly in developing countries, more than 6.5 million tons of sesame seeds were produced from nearly 13 million ha [4]. With good adaptation to drought-prone and marginal environments, it can play an active role in the development of an ecologically and societally resilient, sustainable agriculture. The seeds are being used for an array of products in the food (high-quality oil, tahini paste, cooking and baking) and pharmaceutical industries [5]. Acknowledged as an important functional food, it

is progressively gaining popularity due to the high content in nutritional components with antihypertensive, anticarcinogenic, anti-inflammatory and antioxidative effects [6–8]. Immense progress has been made with continually advancing genomics technologies to decipher and understand crop genomes. For sesame, an orphan crop until recently, despite its long history of cultivation, breeding efforts were mostly concentrated on addressing the low yield (400–500 Kg/ha) [4] that seed shattering, indeterminate growth habit and asynchronous capsule ripening causes [9–13]. In the past few years, sesame came across to the “Omics” era, and as with other crops, a substantial amount of genomics data began to amass [14–16].

However, the impact of genomics data on crop improvement is still far from satisfactory, and our ability to accurately assess crop status in field scale is lacking compared to the current capacity to generate high-throughput genomics data. Thus, the research bottleneck in plant sciences shifts from genotyping to phenotyping. A phenotype is the composite of an observable expression of a genome for traits in a given environment. Traits could be visible to the naked eye (conventional phenotype), or visible by using technical procedures. Phenomics, the systematic genome-wide study of an organism’s phenotype is an emerging approach that aims to automate and standardize phenotyping [17–19]. To mitigate this ‘phenomics bottleneck’, innovations such as trait data recording through sophisticated non-invasive imaging, spectroscopy, satellite image analysis, high-performance computing facilities, phenomics databases, robotics and Artificial Intelligence (AI) have been utilized. The phenomics revolution is here, and the monitoring of thousands of plants in a single day for traits such as plant architecture, photosynthesis ability and biomass productivity made it possible for “speed breeding” to unravel [20–22]. Genetic gain is a fundamental concept in breeding and can be enhanced by increasing selection intensity, accuracy and genetic variation and/or reducing the cycle time. Phenotyping contributes both directly and indirectly to these variables [23], but it comes with a high cost.

Simple active radiometer sensors, on the other hand, may enable phenotyping of field experiments in a rapid and cost-effective way. Remote sensing, through a set of spectral vegetation indices, has been used in breeding trials just recently [24]. Strong associations have been demonstrated between spectral reflectance indices and attributes of crop growth, and the development of new instruments enhances their monitoring [25–29]. Leaf pigments (e.g., carotenoids and anthocyanins) absorb various amounts of light in the visible range of the spectrum. These leaf characteristics influence the reflectance signature of plants. Reflectance measurements made near the crop canopy integrate plant-to-plant variation throughout plant growth cycles, associated with the impacts of senescence or stress conditions (e.g., due to water or nutrient deficits) on the leaf characteristics [30]. Precise non-destructive biomass estimates in breeding programs, could be useful in selection, particularly if they are quick, cheap and easy to perform [24].

The Normalized Difference Vegetation Index (NDVI) is one of the most utilized spectral reflectance indices (SRIs) for indirect selection in breeding programs. Cabrera-Bosquet et al. [28] showed that a spectral vegetation index such as NDVI is a promising tool to screen genotypes. NDVI and other spectral reflectance indices have the potential to differentiate spring wheat genotypes from heading to grain filling stages for crop biomass and grain yield under irrigated conditions [31]. Ma et al. [32] reported that NDVI could differentiate between high and low grain yield among soybean (*Glycine max*, L., Merr.) genotypes. They concluded that NDVI can be a reliable and fast index. Moreover, the reflectance of red light is a good way to quantify plant chlorophyll content until the canopy approaches closure. Once the canopy closes, red light reflectance remains very low and thus is no longer responsive to changes in plant chlorophyll content. Reflectance in the red-edge region of the spectrum has been shown to be quite sensitive to canopy chlorophyll content over a wide range of biomass conditions and thus the value of the normalized difference red edge index (NDRE). Canopy biomass is best quantified by measuring near-infrared (NIR) reflectance. In a practical sense, NIR reflectance quantifies the size of the photosynthetic

factory while red and red-edge reflectance collectively characterize how fast the factory can operate [33,34].

Recent advances in precision agriculture technology have led to the development of ground-based active remote sensors (or crop canopy sensors) that calculate a set of reflectance indices such as NDVI, NDRE and NIR. Active sensors have their own source of light energy and allow for the determination of those indices at specific times and locations throughout the growing season without the need for ambient illumination or flight concerns. Crop canopy sensors are relatively small in size and contain an integrated light source. They operate by directing visible (VIS) light (400–700 nm) as well as near-infrared (NIR) (700–1300 nm) light at the plant canopy of interest [35]. One of the most reliable types of sensors used mainly for scanning crops to make nitrogen (N) fertilizer recommendations, assess forage biomass, estimate yield, estimate crop leaf area and geospatially map agricultural landscapes is the Holland Scientific Crop Circle™ ACS-430 plant canopy reflectance sensor [36–40]. The Crop Circle™ sensor is active and operates under the same principles as that of the GreenSeeker™ sensor; the principles and physics behind the operation of those sensors are described in detail in Inman et al. [40]. The Crop Circle™ sensor generates light with a wavelength of 590 nm in the VIS band and 880 nm in the NIR band. The Crop Circle ACS-430 sensor showed the best results, displaying the greatest range of measured values and the highest sensitivity as a biomass predictor, when used in comparison with other devices in sugarcane [41–43].

In many recent studies, SRIs from proximity sensors were used for early wheat selection breeding cycles [44–47]. Selection in early breeding generation is challenging because the small-size plots and the large number of lines under evaluation do not allow for an accurate determination of the yield, and for this reason breeders typically rely on visual selection.

Moreover, the phenotyping in each crop/variety is significantly affected by the growth stage; thus, many researchers focus on investigating the optimal growth stage of scanning that could be used in the breeding trials. For wheat, a recent study showed that under dryland conditions, there is a reliable correlation between grain yield and NDVI at the early growing season, the anthesis growth stage and the mid-grain filling growth stage, as well as a poor association under irrigated conditions [48]. Relative differences in leaf senescence patterns of soybean cultivars have been studied to accurately calculate the observed maturity rate [49,50].

Using spectral reflectance indices for sesame phenotyping and yield estimation in a breeding program has only been recorded once before [51].

The objectives of this study were to: (1) develop a high-throughput phenotyping workflow to estimate the NDVI and NDRE at the plot-level through the active crop canopy sensor; (2) test the ability of SRIs to distinguish between sesame cultivars throughout the crop growth period; and (3) identify specific stages in the sesame growth cycle that contribute to phenotyping accuracy and functionality.

This article is structured as follows. In Section 2, we will describe the experimental design and the genetic material that we used, the phenotyping workflow that we established and the statistical analysis that was applied. In Section 3, we will present the results for the ability of the SRIs to differentiate sesame genotypes at different stages of their development, and we will unravel the genetics behind the SRIs in single and multi-environments sesame trials. In Section 4, we will discuss if the results of this study showed that we can integrate SRIs and high throughput phenotyping in a sesame breeding scheme. Finally, the article will end with a brief presentation of the conclusions in Section 4 (Figure 1).

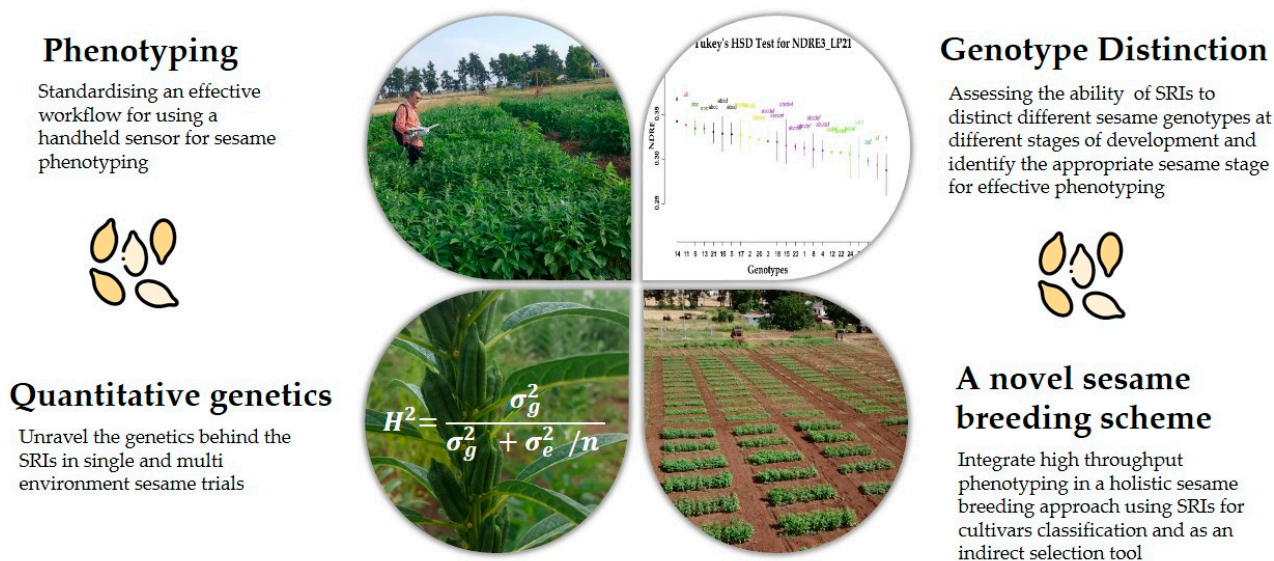


Figure 1. Graphical abstract of the workflow of our study.

2. Materials and Methods

2.1. Experimental Conditions

Field experiments were conducted in 2020 and 2021 at the Institute of Industrial and Forage Crops (IIFC) of the Hellenic Agricultural Organization—DIMITRA (ELGO-DIMITRA) in Larissa (x: 2496060, y: 4809270, Projected Coordinate Systems WGS_1984_Web_Mercator), central Greece (Figure 2). The climate in the region of Larissa is a semi-arid Mediterranean climate and is classified as Csa (temperate climate with a hot-dry summer) by the Köppen–Geiger system [52].



Figure 2. Location map of the research area (left). Plots of sesame, late planting at the front and normal at the back (Right, above). Sesame phenotyping with proximity sensor (Right, below).

Soil physicochemical analyses were provided by the accredited under international quality standards (ELOT EN ISO/IEC 17025, 2017) Soil, Water and Plant Analysis lab of IIFC. Both experiments were carried out on a Vertisol [53] clayey soil (37% sand, 21% silt, 42% clay) with poor organic carbon content (0.36–0.75%) at 30 cm depth. The soil had low carbonate content (1.2%) and electrical conductivity (393 $\mu\text{S}/\text{cm}$), was slightly alkaline in pH (7.4), had high concentrations of K (508 mg/kg), and low Olsen P (18 mg P/kg).

2.2. Experimental Design and Crop Management

To examine the use of a proximity sensor as an in-field phenotyping tool for sesame (*Sesamum indicum* L.) breeding, four experiments occurred on two planting dates for two consecutive years.

Planting for the full-season crop system (normal planting 2020, NP20) was carried out on 11 May 2020, whereas for the double-crop system (late planting 2020, LP20) on 9 June 2020 and in 2021 on 13/5 and 11/6, respectively (NP21 and LP21). For NP, the dates were chosen in such a way to evaluate sesame's rotational fit with other summer crops (cotton) in the region. LP could be useful for determining the utility of sesame in a double crop system with winter crops (cereals, legumes, etc.) or to serve as a rescue crop in case of crop failure.

Field preparation consisted of disking, turning the soil with a moldboard plow, and smoothing the surface with a field cultivator 20 days before sowing. Previous cultivation was sesame. Balanced pre-plant fertilization with 100 kg ha⁻¹ in the form (11-15-15) was incorporated in the soil before sowing. Treatments of 24 sesame genotypes were randomly assigned within each of the four blocks to follow a randomized complete block design with 96 total number of plots for each planting date. Each plot consisted of 4 rows 3 m long with 25 cm row spacing and a seeding rate of 40 seeds per meter. Sprinkler irrigation was applied right after sowing. Manual thinning was performed when the plants reached a height of 10–12 cm, so as to reach a plant population density of 200,000 plants ha⁻¹ (on-row plant spacing of 20 cm). In-season N fertilization was performed at the beginning of the sesame reproductive stage (\approx 50 Days after planting, DAP) by 70 kg ha⁻¹ of nitrogen in the form of nitrate nitrogen (34.5-0-0). Sprinkler irrigation was applied throughout the growing season to sustain plant development. The plots were weeded manually once a week, and phytosanitary actions were performed to keep them free of pests. All the soil and crop management was the same for both planting days (NP and LP) and cropping years (2020, 2021).

2.3. Plant Material

The plant material used in this work included a total of 24 sesame (*Sesamum indicum* L.) genotypes. Seventeen of them were second generation "sister lines", one was a commercial variety from Turkey and six were Greek parental landraces from the IIFC's gene bank with different eco-geographical origin (Table 1). The sister lines were selected from the six landraces during IIFC's sesame breeding project in which single plant selection with honeycomb methodology under low plant density (nil-competition) was the core idea. A field evaluation methodology that is advantageous in relation to the elimination of the masking effects of soil heterogeneity, maximization of phenotypic expression and application of high selection intensity was applied [54–56].

Table 1. List of the 24 sesame genotypes used in the present study. NP: sister line derived from normal planting. LP: sister line derived from late planting. Com: commercial variety. PL: parental landrace. The parental landraces are named after their region of origin. So, our materials are high-rate homozygous lines derived from 5 parental landraces.

GEN	Parental Landrace	GEN	Parental Landrace	GEN	Parental Landrace	GEN	Parental Landrace
1 (NP)	Kilkis	7 (NP)	Kokkina	13 (LP)	Sidirochori	19 (PL)	Ormenio
2 (NP)	Kilkis	8 (NP)	Serres	14 (LP)	Sidirochori	20 (PL)	Kokkina
3 (NP)	Kilkis	9 (NP)	Serres	15 (LP)	Sidirochori	21 (PL)	Sidirochori
4 (NP)	Sidirochori	10 (NP)	Ormenio	16 (LP)	Kokkina	22 (PL)	Serres
5 (NP)	Sidirochori	11 (LP)	Kilkis	17 (LP)	Evros	23 (PL)	Kilkis
6 (NP)	Sidirochori	12 (LP)	Kilkis	18 (Com)	Turkey	24 (PL)	Evros

2.4. Crop Phenotyping

The canopy reflectance of each plot was measured by a single Crop Circle ACS-430 active canopy sensor interfaced to a GeoScout X data logger (Holland Scientific, Lincoln, NE, USA) from a nadir view 0.5 m above the crop canopy several times in the growing period.

Field scans were performed with the sensor mounted on a portable frame, with an average speed of 4 km h⁻¹ e between 8:00 a.m. and 9:30 a.m. local time, spanning the monitoring period from the early reproductive stage to mid-ripening stage. For each plot, 40–50 data points of canopy reflectance were recorded as the average of more than 4000 sensor readings by plot.

For both planting dates and years, monitoring started when all genotypes were at the reproductive stage. The canopy reflectance was measured at 670 nm (R_{RED}), 730 nm ($R_{RED\ EDGE}$) and 780 nm (R_{NIR}) wavelengths. The spectral reflectance data from the three bands were used to derive two vegetation indices: normalized difference vegetation index (NDVI) (1) and normalized difference red edge (NDRE) (2), which were evaluated as potential tools for genotype classification.

$$NDVI = (R_{NIR} - R_{RED}) / (R_{NIR} + R_{RED}) \quad (1)$$

$$NDRE = (R_{NIR} - R_{RED\ EDGE}) / (R_{NIR} + R_{RED\ EDGE}) \quad (2)$$

The data points obtained on each day were later processed to get one average value for each plot. The NDVI is related to crop parameters such as leaf area index, biomass and fractional vegetation cover, whereas the NDRE characterizes the chlorophyll/nitrogen status of crop canopies.

The soil plant analysis development (SPAD), an index for chlorophyll content, recorded at the beginning of the reproductive stage with the CCM-200 plus SPAD-meter from five randomly selected plants of each plot.

Seed yield (kg/ha) was assessed at the harvest maturity stage of each cultivar. The two central rows from each plot were harvested by hand, threshed with a Wintersteiger LD 350 laboratory thresher, and the seed produced was weighed.

All the trait measurements were taken from the two central rows in each plot to avoid edge effects.

2.5. Growing Degree Days and Weather Parameters

Growing degree day (GDD) values specific for sesame were calculated for each day during the growing season for both planting days. Data on air temperature, precipitation, relative humidity and solar radiation were acquired from the automatic meteorological station that the IIFC operates in collaboration with the National Observatory of Athens (IERSD) in its experimental fields. The following equation was used to calculate daily GDD values (3):

$$GDD = [(T_{MIN} + T_{MAX}) / 2] - T_b = T_{AVG} - T_b \quad (3)$$

where T_{MIN} and T_{MAX} are the daily minimum and maximum temperatures, T_{AVG} is the daily average temperature, and T_b is the base temperature for sesame. Angus et al. [57] demonstrated in their study the value of a linear day-degree system for predicting crop phasic development, modeled the response of 44 species to temperature and presented their respective base temperatures. For sesame, it was 15.9 °C, and we used it as T_b [58]. On days when T_{AVG} was below T_b , the GDDs for that day were set to 0. Daily GDDs were separately summed to calculate the accumulated GDD value from sowing to harvest.

2.6. Statistical Analysis

The R-program (www.R-project.org, accessed on 7 February 2022) with the packages Metan and Agricolae were used to perform all the statistical analysis [59–61].

An analysis of variance (ANOVA) including the factors sesame line and block was performed on data of separate growing conditions (NP and LP) and cropping years to verify

the occurrence of genetic variation among lines for each trait. If significant differences were found, Tukey's HSD (honestly significant difference) method was used for multiple comparisons ($\alpha = 5\%$). The phenotypic (rp) (5) and genotypic correlation (rg) (4) coefficients between spectral indices and the grain yield were calculated using the following formulas [62]:

$$rg_{xy} = \frac{Cov_{gxy}}{\sqrt{(\sigma_{gx}^2)(\sigma_{gy}^2)}} \quad (4)$$

$$rp_{xy} = \frac{Cov_{pxy}}{\sqrt{(\sigma_{px}^2)(\sigma_{py}^2)}} \quad (5)$$

where σ^2g/σ^2p and $Covg/Covp$ refer to the components of genetic and phenotypic variance and covariance, respectively, and X and Y are the two variables.

Broad-sense heritability (H^2) was calculated on a line mean basis for each environment (cropping years, NP, LP) according to Holland [63]. Broad-sense heritability is the proportion of the phenotypic variance, which is explained by the genetic variance, and was estimated as follows (6):

$$H^2 = \frac{\sigma_g^2}{\sigma_g^2 + \sigma_e^2/n} \quad (6)$$

where σ^2g and σ^2e are the genotypic and residual variance components, respectively, and n is the number of replicated blocks. Relative efficiency of indirect selection (E_r) in SRIs vs. direct selection in yield expressed in percentage, was estimated by the following equation [64] (7):

$$E_r = [(H_{SRI}/H_Y)rg_{SRI Y}] \times 100 \quad (7)$$

where H_{SRI} and H_Y are the square root of the broad-sense heritability on a line mean basis (H^2) for the SRIs and Yield, respectively, and $rg_{SRI Y}$ is the genetic correlation between the two criteria. Restricted maximum likelihood with best linear unbiased prediction (REML/BLUP) is a well-known linear mixed model for the estimation of random effects that was used to analyze the SRIs data from every environment (cropping years, NP, LP). The output was p -values from Likelihood Ratio Test (LRT) of the analyzed SRIs for genotype (GEN) and genotype-vs-environment (GE) as random effects. Broad-sense heritability (H_x^2) (8) on a plot basis over the environments (cropping years, NP, LP) and broad-sense heritability (H_y^2) (9) on an entry mean basis over the environments were also estimated.

$$H_x^2 = \frac{\sigma_g^2}{\sigma_g^2 + \sigma_{ge}^2 + \sigma_e^2} \quad (8)$$

$$H_y^2 = \frac{\sigma_g^2}{\sigma_g^2 + \frac{\sigma_{ge}^2}{e} + \frac{\sigma_e^2}{en}} \quad (9)$$

where σ_{ge}^2 refer to the variance component relative to GE interaction and e and n are the number of environments and blocks, respectively.

Hierarchical cluster analysis was performed also to compute the Euclidean distances between the genotypes based on the SRIs with the unweighted pair group with arithmetic mean agglomeration method (UPGMA). Mantel's test was used to check the relationships between the distance matrices when the clustering was performed for separate growing conditions (NP and LP) and cropping years.

3. Results

3.1. Climate Data

Air temperature during the growing season was similar for both growing conditions (NP and LP) and cropping years (2020, 2021), with daily averages being >15.9 °C (Tb) almost for the entire season (Figure 3). The harvest for all plots was completed on 15 September (127 DAP) for normal planting and 19 October (132 DAP) for late planting in 2020 and on 22 September (132 DAP) and 19 October (130 DAP) in 2021.

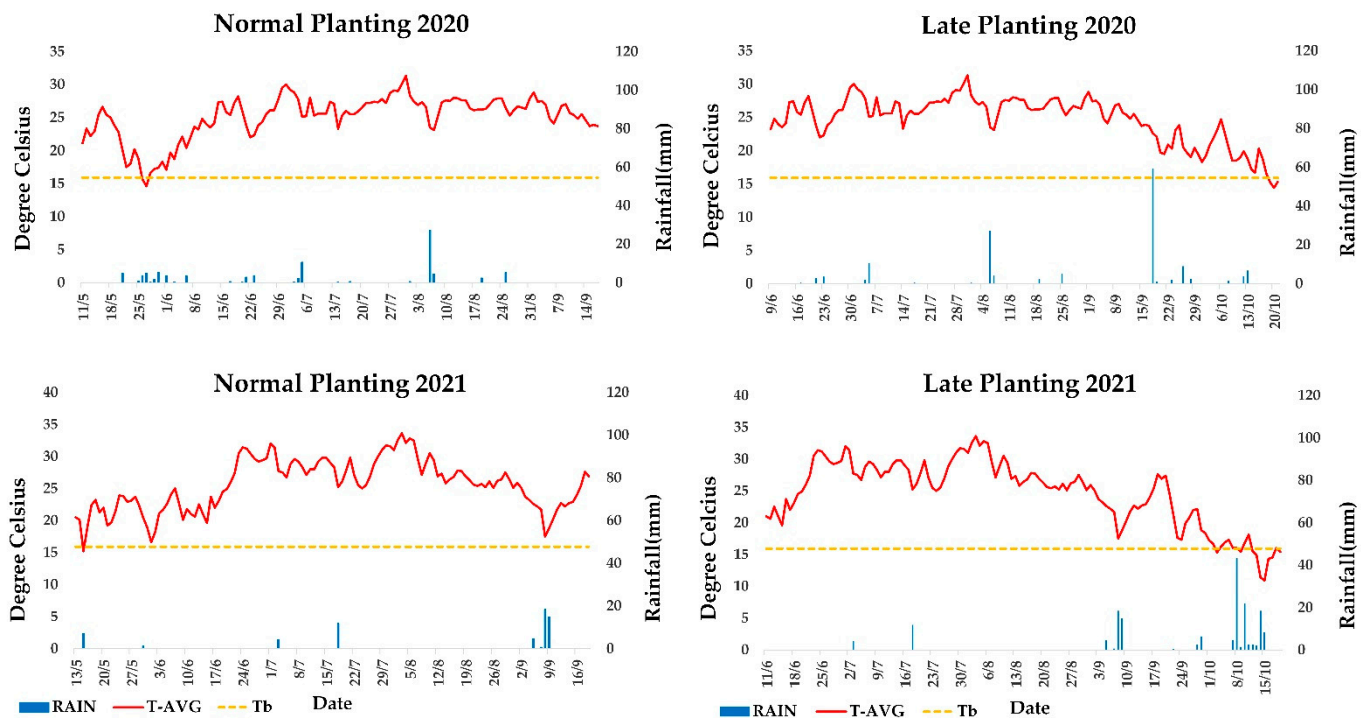


Figure 3. Climate data across growing conditions and years (NP20, LP20, NP21, LP21). Daily Precipitation (RAIN), daily average air temperature (T-AVG), base temperature for sesame (Tb).

Accumulated GDDs over the growing period were the same for both planting dates (8.8 and 8.6 GDD day⁻¹ for 2020 and 2021, respectively); however, the accumulation rate in LP was lower in comparison with NP (9.2 and 9.5 GDD day⁻¹ for 2020 and 2021) (Figure 3). Only two important rainfall events occurred (18 September 2020, 59.2 mm and 8 October 2021, 43.2 mm). The amount of solar radiation received was 2% and 11% higher in NP than LP for 2020 and 2021, respectively. As expected for the late planting, in both years lower temperature and solar radiation with higher RH% and rainfall during the ripening stage resulted in more days for plant maturity and delayed harvest especially in 2021 (Table 2).

Table 2. Accumulated growing degree days (GDDs) over the sesame growing season (from planting to harvest), accumulated rainfall and irrigation (mm) and accumulated solar radiation (W m⁻²) for both planting dates and years.

Cummulative Total	NP 2020	NP 2021	LP 2020	LP 2021
GDD	1196	1265	1191	1133
Rainfall (mm)	89.6	63.2	147.6	168.4
Irrigation (mm)	275	295	200	240
Solar radiation (Wm ⁻²)	65,158	67,332	63,634	60,109

3.2. Sesame Phenotyping

Continuous measurements from the beginning of the reproductive stage and almost once a week until the end of the ripening stage enabled genotype comparisons (Table 3, Figures 4 and 5).

The examined sesame genotypes (lines and parental landraces) can be divided into two large groups, the early and very early maturing (1, 8, 9, 10, 17, 18, 19, 20, 22, 23, 24) and intermediate to late maturing (2, 3, 4, 5, 6, 7, 11, 12, 13, 14, 15, 16, 21) with different rates of development.

Table 3. Temporal distribution of the proximal sensing data during the sesame growing period.

	Scan Date	DAP	GDD	GS		Scan Date	DAP	GDD	GS
SCAN 1	1 July 2020	51	359	RES	NP 2020	3 August 2020	55	591	RES
SCAN 2	13 July 2020	63	488	RES		10 August 2020	62	661	RES
SCAN 3	24 July 2020	74	601	RES		25 August 2020	77	829	RES
SCAN 4	3 August 2020	84	727	RES		2 September 2020	85	917	RES
SCAN 5	10 August 2020	91	797	RES		11 September 2020	94	1007	RES
SCAN 6	25 August 2020	106	965	RIS		22 September 2020	105	1083	RES
SCAN 7	2 September 2020	114	1053	RIS		9 October 2020	122	1169	RIS
SCAN 1	2 July 2021	50	373	RES	NP 2021	28 July 2021	47	514	RES
SCAN 2	13 July 2021	61	508	RES		9 August 2021	59	698	RES
SCAN 3	21 July 2021	69	607	RES		20 August 2021	70	825	RES
SCAN 4	28 July 2021	76	684	RES		27 August 2021	77	904	RES
SCAN 5	9 August 2021	88	868	RES		3 September 2021	84	962	RES
SCAN 6	20 August 2021	99	995	RES		10 September 2021	91	997	RES
SCAN 7	27 August 2021	106	1063	RIS		17 September 2021	98	1047	RES
SCAN 8	3 September 2021	113	1132	RIS		27 September 2021	108	1113	RIS
SCAN 9						5 October 2021	116	1128	RIS

DAP = days after planting, GDD = growth degree days, GS = growth stage, RES = reproductive stage, RIS = ripening stage.

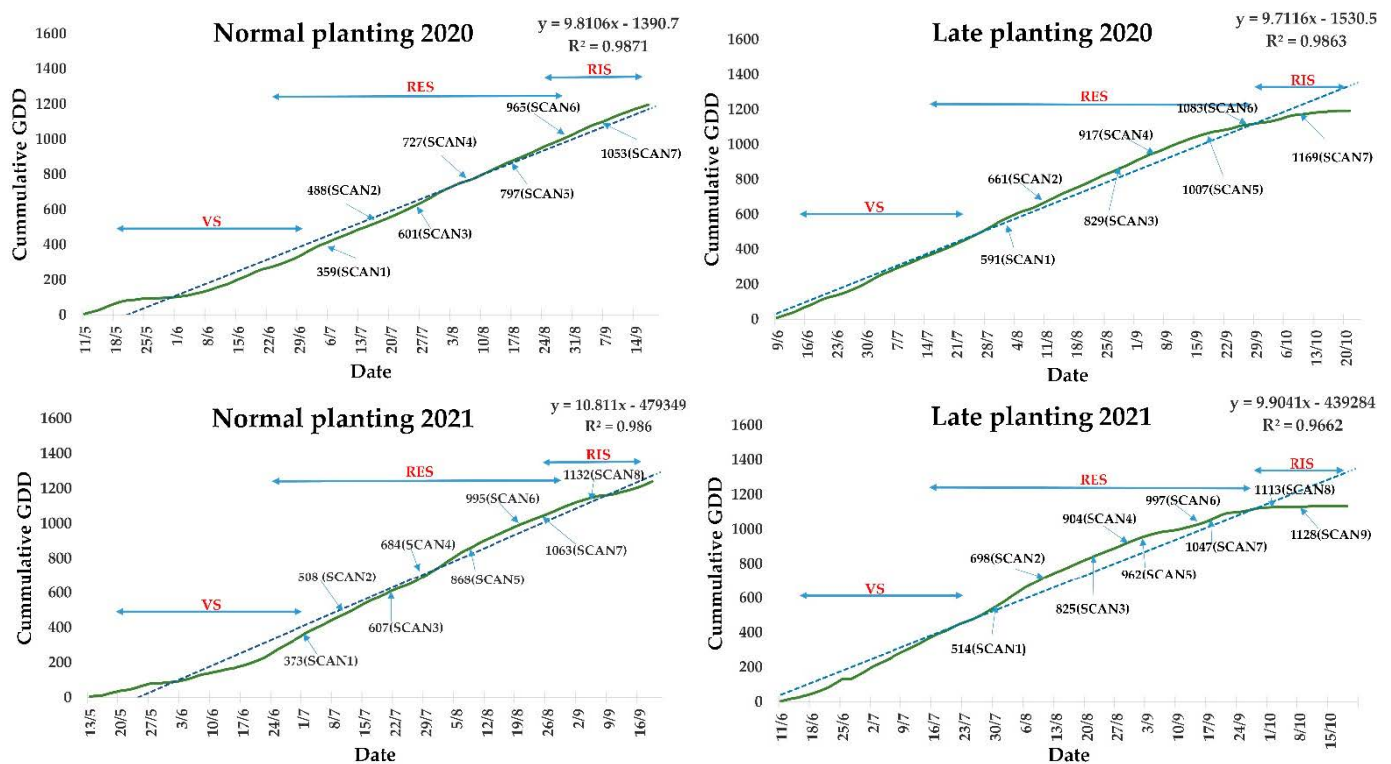


Figure 4. Pattern of GDD accumulation rates for both growing conditions and cropping years. Shown is the fitted linear regression line for the GDD parameters, along with the equations and R^2 . Scanning dates in dependence with GDD and sesame phenology phases (VS = vegetative stage, RES = reproductive stage, RIS = ripening stage).

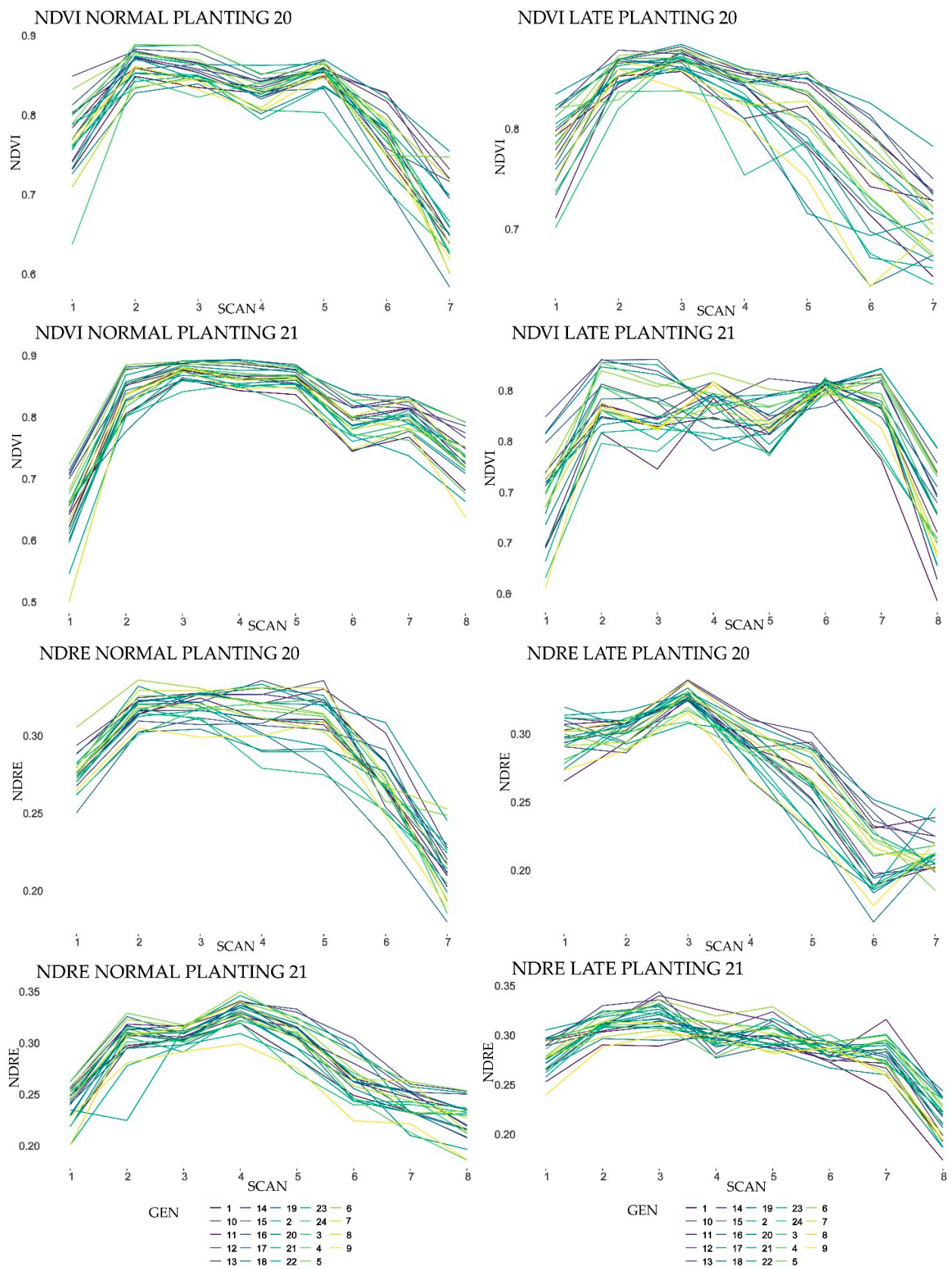


Figure 5. Line graphs from field phenotyping. NDVI and NDRE values of sesame lines and landraces (GEN) for both growing conditions and cropping years monitored by Crop Circle ACS-430 active canopy sensor. (x axis = number of scans, y axis = SRI values for each genotype).

NDVI values ranged from 0.424 to 0.902 with an all-genotypes average of 0.782. A common pattern of NDVI evolution was observed for almost all of the genotypes. NDVI had the lowest value at the first scan (51 DAP) in the beginning of the reproductive stage, reaching the maximum values at 2, 3, 4 scans followed by a progressive decline in accordance with the maturity of the crop. From scan 1 to 2 when also the in-season N fertilization occurred, the NDVI average values for all genotypes increased from 0.75 to 0.85 (approximately by 13%). NDVI values remained almost in variable for scans 2 to 5 until the crop entered ripening stage. For NP21, the NDVI raise from scan 1 to 2 was from 0.65 to 0.85.

Similar patterns were observed for the NDRE. Its values ranged from 0.130 to 0.360 with an all-genotypes average of 0.267. From scan 1 to 2 NDRE average values for all genotypes increased from 0.28 to 0.31 (approximately by 10%) except NP21 when as in the case of NDVI average values showed a steep raise. The decline was rapid for both indices, but for NDRE, it started earlier when the crop was still in the reproductive stage. (Figure 4). Variation between sesame lines was greater for both indices in LP20 and NP21. NDVI varied significantly between genotypes for every monitoring date in both growing conditions and cropping years and almost the same was observed for NDRE, except scans 1 and 6 on NP20 and scan 9 on LP20. Both NDVI and NDRE enabled distinction between genotypes but in most cases NDVI provided better separation, as shown at four monitoring dates during crop growth (Tables 4–6). Even in the middle of the reproductive growth stage when crop canopy is closed (NDVI3, LP21 and NDRE3, LP21) SRI values produced a clear genotype separation (Figure 6, genotypes with different letter and color are significant different). Line 2 gave the higher NDRE and NDVI values (mean values from both planting dates and years) 0.282 and 0.822, respectively, lines 1 and 9 had the lowest values (0.250 and 0.750), respectively. Early maturing lines and landraces always had low NDVI, but NDRE produced mixed results and even late maturing lines exhibited low values.

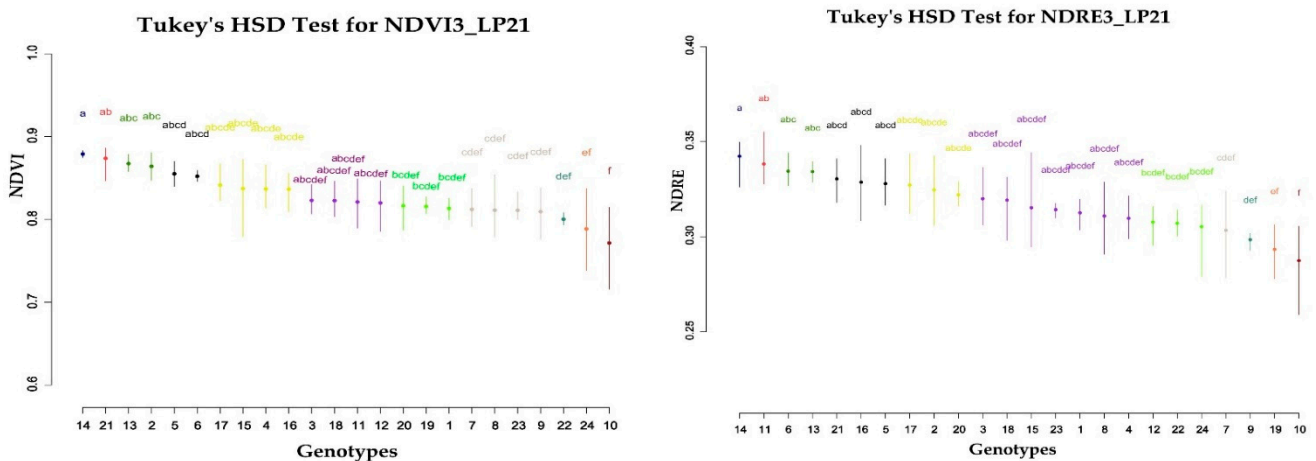


Figure 6. Tukey’s HSD separation procedure for NDVI and NDRE of the third monitoring date for the LP in 2021. Groups and range (genotypes with the same letter are not significant different).

Table 4. Average NDVI index value by genotype at four monitoring dates. The specific monitoring covers the period from the middle of the reproductive stage till the beginning of the ripening stage. Means and ANOVA F values to verify the occurrence of genetic variation among lines for each SRI.

GEN	NP20				NP21				LP20				LP21																			
	NDVI3	NDVI4	NDVI5	NDVI6																												
1	0.833	cd	0.825	ab	0.847	ab	0.748	abc	0.859	ab	0.840	e	0.834	de	0.743	bc	0.875	a	0.842	abc	0.780	defg	0.712	efghij	0.813	bcdef	0.822	bcde	0.805	a	0.824	c
2	0.886	a	0.849	ab	0.868	a	0.819	ab	0.881	a	0.873	abcde	0.875	abc	0.836	a	0.883	a	0.859	a	0.848	ab	0.824	a	0.864	abc	0.842	abcd	0.844	a	0.867	a
3	0.821	d	0.839	ab	0.855	a	0.784	abc	0.875	a	0.866	abcde	0.866	abcd	0.798	abc	0.836	b	0.826	abc	0.808	abcdef	0.723	defghi	0.823	abcdef	0.836	abcd	0.832	a	0.862	ab
4	0.861	abcd	0.837	ab	0.854	a	0.769	abc	0.876	a	0.869	abcde	0.863	abcd	0.770	abc	0.869	ab	0.845	abc	0.836	abcd	0.762	abcdefg	0.837	abcde	0.820	bcde	0.819	a	0.865	ab
5	0.886	ab	0.850	ab	0.854	a	0.747	abc	0.888	a	0.886	ab	0.878	abc	0.825	abc	0.878	a	0.847	ab	0.856	a	0.795	abcd	0.855	abcd	0.846	abc	0.833	a	0.868	a
6	0.868	abcd	0.825	ab	0.865	a	0.788	abc	0.883	a	0.885	ab	0.878	abc	0.794	abc	0.878	a	0.858	a	0.834	abcd	0.782	abcde	0.852	abcd	0.866	a	0.850	a	0.868	a
7	0.844	abcd	0.829	ab	0.844	ab	0.792	abc	0.879	a	0.860	abcde	0.862	abcd	0.777	abc	0.865	ab	0.847	ab	0.801	abcdef	0.731	cdefghi	0.812	cdef	0.834	abcd	0.811	a	0.846	abc
8	0.841	abcd	0.807	ab	0.863	a	0.769	abc	0.877	a	0.857	abcde	0.860	abcd	0.798	abc	0.856	ab	0.822	abc	0.826	abcd	0.755	abcdefgh	0.811	cdef	0.854	ab	0.809	a	0.854	abc
9	0.830	cd	0.802	ab	0.849	a	0.746	abc	0.871	ab	0.844	e	0.846	bcde	0.745	abc	0.837	b	0.805	c	0.749	fgh	0.641	j	0.809	cdef	0.857	ab	0.815	a	0.850	abc
10	0.851	abcd	0.821	ab	0.847	ab	0.776	abc	0.874	a	0.858	abcde	0.862	abcd	0.798	abc	0.856	ab	0.809	bc	0.821	abcde	0.741	bcdefghi	0.772	f	0.841	abcd	0.787	a	0.844	abc
11	0.841	abcd	0.834	ab	0.857	a	0.815	ab	0.879	a	0.864	abcde	0.864	abcd	0.793	abc	0.867	ab	0.853	a	0.844	abc	0.792	abcde	0.821	abcdef	0.857	ab	0.820	a	0.873	a
12	0.856	abcd	0.841	ab	0.856	a	0.825	a	0.873	a	0.865	abcde	0.852	abcde	0.814	abc	0.873	a	0.855	a	0.832	abcd	0.774	abcdef	0.820	abcdef	0.845	abc	0.806	a	0.847	abc
13	0.863	abcd	0.840	ab	0.866	a	0.752	abc	0.889	a	0.884	abc	0.875	abc	0.835	ab	0.881	a	0.855	a	0.848	ab	0.794	abcd	0.867	abc	0.836	abcd	0.860	a	0.864	ab
14	0.864	abcd	0.840	ab	0.852	a	0.826	a	0.885	a	0.891	a	0.883	a	0.817	abc	0.877	a	0.845	abc	0.853	a	0.808	abc	0.879	a	0.825	abcde	0.844	a	0.863	ab
15	0.877	abc	0.844	ab	0.852	a	0.756	abc	0.889	a	0.889	a	0.873	abc	0.812	abc	0.868	ab	0.844	abc	0.849	ab	0.812	ab	0.837	abcde	0.857	ab	0.823	a	0.861	ab
16	0.862	abcd	0.818	ab	0.848	a	0.799	abc	0.884	a	0.880	abcd	0.870	abc	0.797	abc	0.860	ab	0.841	abc	0.808	abcdef	0.755	abcdefg	0.837	abcde	0.789	e	0.812	a	0.834	bc
17	0.854	abcd	0.828	ab	0.831	ab	0.708	bc	0.871	ab	0.861	abcde	0.850	abcde	0.741	c	0.864	ab	0.808	bc	0.721	gh	0.642	j	0.841	abcde	0.812	cde	0.816	a	0.840	abc
18	0.837	bcd	0.800	b	0.835	ab	0.781	abc	0.862	ab	0.846	de	0.852	abcde	0.785	abc	0.867	ab	0.842	abc	0.784	cdef	0.718	defghij	0.823	abcdef	0.821	bcde	0.812	a	0.853	abc
19	0.846	abcd	0.824	ab	0.858	a	0.771	abc	0.858	ab	0.852	bcde	0.857	abcd	0.783	abc	0.858	ab	0.829	abc	0.790	bcdef	0.696	fghij	0.816	bcdef	0.843	abc	0.825	a	0.852	abc
20	0.842	abcd	0.831	ab	0.855	a	0.729	abc	0.865	ab	0.861	abcde	0.860	abcd	0.767	abc	0.860	ab	0.827	abc	0.714	h	0.692	ghij	0.816	bcdef	0.800	de	0.806	a	0.841	abc
21	0.862	abcd	0.860	a	0.862	a	0.781	abc	0.889	a	0.891	a	0.880	ab	0.824	abc	0.870	ab	0.849	ab	0.836	abcd	0.772	abcdefg	0.874	ab	0.833	abcd	0.843	a	0.870	a
22	0.848	abcd	0.821	ab	0.853	a	0.765	abc	0.871	ab	0.849	de	0.851	abcde	0.778	abc	0.858	ab	0.829	abc	0.778	defg	0.670	ij	0.800	def	0.846	abc	0.796	a	0.849	abc
23	0.848	abcd	0.792	b	0.833	ab	0.781	abc	0.839	b	0.850	cde	0.844	cde	0.758	abc	0.869	ab	0.834	abc	0.763	efgh	0.674	hij	0.811	cdef	0.806	cde	0.787	a	0.823	c
24	0.847	abcd	0.804	ab	0.801	b	0.703	c	0.857	ab	0.847	de	0.817	e	0.767	abc	0.875	a	0.836	abc	0.786	cdef	0.729	cdefghi	0.789	ef	0.834	abcd	0.785	a	0.823	c
MEAN	0.853		0.828		0.850		0.772		0.874		0.865		0.861		0.790		0.866		0.838		0.807		0.741		0.828		0.834		0.818		0.852	
Fvalue	8.42	***	2.93	***	3.33	***	2.45	NS	4.74	***	6.48	***	6.19	***	2.99	***	3.71	***	4.46	***	14	***	12.4	***	5.02	***	3.94	***	3.05	***	1.95	**

Within column and year, means followed by the same letter are not significantly different using Tukey HSD separation procedure. ** = $p < 0.05$, *** = $p < 0.01$.

Table 5. Average NDRE index value by genotype at four monitoring dates. The specific monitoring covers the period from the middle of the reproductive stage till the beginning of the ripening stage. Means and ANOVA F values to verify the occurrence of genetic variation among lines for each SRI.

GEN	NP20				NP21				LP20				LP21			
	NDRE3	NDRE4	NDRE5	NDRE6	NDRE3	NDRE4	NDRE5	NDRE6	NDRE3	NDRE4	NDRE5	NDRE6	NDRE3	NDRE4	NDRE5	NDRE6
1	0.315 abc	0.315 abc	0.310 abc	0.266 a	0.302 ab	0.318 bcd	0.284 bcd	0.248 abc	0.324 abc	0.293 ab	0.251 bcd	0.188 abcde	0.313 abcdef	0.303 abcd	0.294 abc	0.275 ab
2	0.327 ab	0.327 ab	0.319 abc	0.307 a	0.308 ab	0.335 abc	0.317 ab	0.291 ab	0.330 abc	0.307 a	0.289 ab	0.251 a	0.325 abcde	0.293 bcd	0.309 abc	0.281 ab
3	0.317 abc	0.317 abc	0.323 ab	0.272 a	0.300 ab	0.330 abc	0.306 abcd	0.269 abc	0.316 abc	0.291 ab	0.262 abcd	0.186 bcde	0.320 abcdef	0.311 abc	0.306 abc	0.293 ab
4	0.316 abc	0.316 abc	0.311 abc	0.264 a	0.299 ab	0.320 abcd	0.309 abc	0.245 abc	0.308 bc	0.285 ab	0.263 abcd	0.222 abcde	0.310 abcdef	0.277 d	0.301 abc	0.281 ab
5	0.325 ab	0.325 ab	0.313 abc	0.257 a	0.316 a	0.338 ab	0.323 a	0.286 ab	0.318 abc	0.286 ab	0.289 ab	0.228 abcd	0.328 abcd	0.301 abcd	0.306 abc	0.282 ab
6	0.330 a	0.330 a	0.313 abc	0.269 a	0.314 ab	0.348 a	0.318 ab	0.272 abc	0.326 abc	0.300 ab	0.285 ab	0.220 abcde	0.334 abc	0.318 ab	0.327 a	0.296 ab
7	0.319 abc	0.319 abc	0.302 abc	0.266 a	0.309 ab	0.325 abcd	0.302 abcd	0.257 abc	0.330 abc	0.295 ab	0.265 abc	0.211 abcde	0.303 cdef	0.292 bcd	0.282 c	0.260 b
8	0.328 a	0.328 a	0.330 a	0.273 a	0.313 ab	0.339 ab	0.310 abc	0.264 abc	0.337 ab	0.304 a	0.275 abc	0.216 abcde	0.311 abcdef	0.313 ab	0.299 abc	0.280 ab
9	0.298 c	0.298 c	0.308 abc	0.247 a	0.290 b	0.298 d	0.274 cd	0.223 c	0.315 abc	0.266 b	0.229 cd	0.173 de	0.298 def	0.298 abcd	0.280 c	0.268 ab
10	0.323 ab	0.323 ab	0.306 abc	0.265 a	0.304 ab	0.324 abcd	0.313 ab	0.261 abc	0.324 abc	0.289 ab	0.274 abc	0.230 abcd	0.287 f	0.302 abcd	0.289 abc	0.283 ab
11	0.326 ab	0.326 ab	0.329 a	0.301 a	0.314 ab	0.333 abc	0.314 ab	0.264 abc	0.338 a	0.311 a	0.291 ab	0.231 abcd	0.338 ab	0.325 a	0.313 abc	0.304 a
12	0.326 ab	0.326 ab	0.320 abc	0.283 a	0.305 ab	0.328 abcd	0.305 abcd	0.279 abc	0.325 abc	0.300 ab	0.263 abcd	0.196 abcde	0.308 bcdef	0.295 abcd	0.286 bc	0.272 ab
13	0.325 ab	0.325 ab	0.335 a	0.253 a	0.316 a	0.339 ab	0.328 a	0.303 a	0.337 ab	0.309 a	0.300 a	0.248 ab	0.334 abc	0.303 abcd	0.322 ab	0.290 ab
14	0.306 abc	0.306 abc	0.322 ab	0.282 a	0.300 ab	0.338 abc	0.331 a	0.291 ab	0.326 abc	0.288 ab	0.293 ab	0.236 abcd	0.342 a	0.279 cd	0.313 abc	0.284 ab
15	0.321 abc	0.321 abc	0.322 ab	0.264 a	0.301 ab	0.338 abc	0.304 abcd	0.261 abc	0.327 abc	0.299 ab	0.287 ab	0.241 abc	0.315 abcdef	0.298 abcd	0.298 abc	0.276 ab
16	0.310 abc	0.310 abc	0.303 abc	0.290 a	0.307 ab	0.335 abc	0.314 ab	0.266 abc	0.328 abc	0.290 ab	0.259 abcd	0.193 abcde	0.329 abcd	0.276 d	0.288 abc	0.274 ab
17	0.320 abc	0.320 abc	0.277 bc	0.233 a	0.310 ab	0.330 abc	0.304 abcd	0.242 bc	0.330 abc	0.265 b	0.227 cd	0.161 e	0.327 abcde	0.287 bcd	0.297 abc	0.281 ab
18	0.303 bc	0.303 bc	0.291 abc	0.276 a	0.297 ab	0.320 abcd	0.304 abcd	0.254 abc	0.323 abc	0.288 ab	0.246 bcd	0.182 cde	0.319 abcdef	0.297 abcd	0.306 abc	0.302 a
19	0.325 ab	0.325 ab	0.325 a	0.264 a	0.308 ab	0.326 abcd	0.294 abcd	0.261 abc	0.333 abc	0.291 ab	0.250 bcd	0.194 abcde	0.293 ef	0.296 abcd	0.285 bc	0.272 ab
20	0.318 abc	0.318 abc	0.292 abc	0.267 a	0.301 ab	0.333 abc	0.313 ab	0.266 abc	0.328 abc	0.278 ab	0.216 d	0.185 bcde	0.322 abcde	0.290 bcd	0.299 abc	0.295 ab
21	0.326 ab	0.326 ab	0.318 abc	0.282 a	0.313 ab	0.345 ab	0.322 ab	0.297 ab	0.307 c	0.300 ab	0.281 ab	0.226 abcd	0.330 abcd	0.291 bcd	0.315 abc	0.294 ab
22	0.315 abc	0.315 abc	0.308 abc	0.265 a	0.297 ab	0.308 cd	0.284 bcd	0.242 bc	0.323 abc	0.279 ab	0.231 cd	0.184 cde	0.307 bcdef	0.304 abcd	0.289 abc	0.281 ab
23	0.309 abc	0.309 abc	0.289 abc	0.249 a	0.290 b	0.324 abcd	0.293 abcd	0.244 abc	0.325 abc	0.286 ab	0.230 cd	0.188 abcde	0.314 abcdef	0.288 bcd	0.289 abc	0.279 ab
24	0.310 abc	0.310 abc	0.274 c	0.251 a	0.303 ab	0.318 abcd	0.269 d	0.238 bc	0.330 abc	0.301 ab	0.260 abcd	0.209 abcde	0.305 bcdef	0.300 abcd	0.290 abc	0.276 ab
MEAN	0.318	0.318	0.310	0.269	0.305	0.329	0.306	0.263	0.325	0.292	0.263	0.208	0.317	0.297	0.299	0.282
Fvalue	3.76 ***	3.24 ***	3.78 ***	1.41 NS	2.55 ***	4.48 ***	5.03 ***	3.5 ***	2.68 ***	3.21 ***	8.29 ***	4.48 ***	5.02 ***	3.94 ***	3.05 ***	1.95 **

Within column and year, means followed by the same letter are not significantly different using Tukey HSD separation procedure. ** = $p < 0.05$, *** = $p < 0.01$.

Table 6. ANOVA F values to verify genetic variation among lines for each SRI, phenotypic correlation(rp) and genotypic correlation(rg) between sesame yield and SRIs, broad-sense heritability on a line mean basis (H²) all on different monitoring dates across growing conditions and cropping years (NP20, NP21, LP20, LP21). Relative efficiency of indirect selection (E_r) in SRIs vs. direct selection in yield expressed in percentage.

SRI	NP 2020						NP2021						LP2020						LP2021													
	Fvalue	rp	rg	H ²	E _r (%)	Fvalue	rp	rg	H ²	E _r (%)	Fvalue	rp	rg	H ²	E _r (%)	Fvalue	rp	rg	H ²	E _r (%)												
NDRE1	1.47	NS	−0.063	NS	−0.038	NS	0.322	−2	2.16	**	−0.363	NS	−0.564	**	0.538	−45	2.59	**	0.291	*	0.369	NS	0.614	31	2.69	**	−0.067	NS	−0.084	NS	0.628	−7
NDRE2	2.43	**	0.214	NS	0.312	NS	0.589	25	2.59	**	0.076	NS	0.108	NS	0.613	9	2.42	**	−0.105	NS	−0.175	NS	0.586	−15	2.30	**	−0.053	NS	−0.088	NS	0.565	−7
NDRE3	3.76	**	0.354	*	0.442	*	0.734	39	2.55	**	0.285	*	0.322	NS	0.608	27	2.68	**	0.134	NS	0.196	NS	0.627	17	5.02	**	−0.015	NS	−0.027	NS	0.801	−3
NDRE4	3.25	**	0.593	**	0.703	**	0.692	60	4.48	**	0.116	NS	0.111	NS	0.777	11	3.21	**	0.235	**	0.218	NS	0.689	20	3.94	**	0.379	**	0.450	*	0.746	40
NDRE5	3.78	**	0.591	**	0.686	**	0.735	61	5.03	**	0.240	*	0.264	NS	0.801	26	8.29	**	0.368	**	0.381	NS	0.879	39	3.05	**	0.002	NS	−0.011	NS	0.672	−1
NDRE6	1.41	NS	0.398	*	0.748	**	0.292	42	3.50	**	0.195	NS	0.276	NS	0.715	25	4.48	**	0.353	*	0.415	*	0.777	40	1.95	*	−0.051	NS	−0.112	NS	0.487	−8
NDRE7	2.22	**	0.197	NS	0.274	NS	0.550	21	2.19	**	0.175	NS	0.335	NS	0.544	27	1.81	*	−0.046	NS	−0.037	NS	0.447	−3	2.55	**	−0.069	NS	−0.084	NS	0.607	−7
NDRE8									2.86	**	−0.058	NS	0.028	NS	0.651	2									3.56	**	−0.379	**	−0.448	*	0.719	−39
NDRE9																								1.68	NS	−0.354	NS	−0.569	**	0.405	−37	
NDVI1	3.34	**	0.104	NS	0.158	NS	0.701	14	2.28	**	−0.276	NS	−0.420	*	0.562	−34	1.80	*	0.444	**	0.660	**	0.446	48	2.04	*	0.084	NS	0.124	NS	0.509	9
NDVI2	4.98	**	0.193	NS	0.227	NS	0.799	21	4.46	**	0.359	**	0.389	NS	0.776	37	2.14	**	0.456	**	0.591	**	0.533	47	3.44	**	0.067	NS	0.053	NS	0.709	5
NDVI3	3.42	**	0.115	NS	0.165	NS	0.708	14	4.74	**	0.434	**	0.470	*	0.789	45	3.71	**	0.090	NS	0.074	NS	0.731	7	5.60	**	−0.033	NS	−0.045	NS	0.821	−4
NDVI4	2.93	**	0.186	NS	0.195	NS	0.658	16	6.48	**	0.181	NS	0.172	NS	0.846	17	4.46	**	0.225	*	0.209	NS	0.776	20	6.15	**	0.428	**	0.468	*	0.837	44
NDVI5	3.33	**	0.538	**	0.654	**	0.700	57	6.19	**	0.391	**	0.415	*	0.838	41	14.00	**	0.334	**	0.359	NS	0.928	38	2.56	**	0.092	NS	0.092	NS	0.609	7
NDVI6	2.45	**	0.273	NS	0.386	NS	0.593	31	2.99	**	0.291	NS	0.379	NS	0.666	33	12.40	**	0.343	*	0.392	NS	0.919	41	5.83	**	0.208	*	0.202	NS	0.829	19
NDVI7	2.81	**	0.258	NS	0.320	NS	0.645	27	3.01	**	0.290	NS	0.399	NS	0.668	35	3.52	**	0.429	*	0.561	**	0.716	52	4.61	**	0.165	NS	0.157	NS	0.783	14
NDVI8									3.26	**	0.025	NS	0.080	NS	0.694	7									4.24	**	−0.127	NS	−0.168	NS	0.764	−15
NDVI9																								3.27	**	−0.089	NS	−0.137	NS	0.694	−12	
SPAD	3.31	**	−0.500	**	−0.623	**	0.698	−54	1.68	NS	−0.324	NS	−0.508	*	0.405	−35	3.31	**	−0.261	NS	−0.323	NS	0.698	−29	1.10	NS	−0.277	NS	−0.914	**	0.095	−29
YIELD	15.80	**	1	**	1	**	0.937		6.98	**	1	**	1	**	0.857		6.55	**	1	**	1	**	0.847		13.60	**	1	**	1	**	0.963	

NS = non-significant * = $p < 0.05$, ** = $p < 0.01$.

3.3. Phenotypic and Genetic Correlations, SRIs with Sesame Yield

NDRE showed strong and significant phenotypic correlations with sesame yield when phenotyping occurred at late reproductive growing stages (scans 3, 4, 5, 6) for both planting dates in 2020 (scan 3/LP for 2020 excluded) but in 2021 only at scan 3/NP, scan 5/NP and scan 4/LP. Genetic correlations between NDRE and yield were similar to phenotypic correlations; however, the coefficients of genetic correlation were generally higher than those of the phenotypic correlations. NDRE genetic correlation values ranged from -0.379 to 0.593 and from -0.564 to 0.748 for r_p and r_g , respectively.

NDVI at scan 5 showed strong and significant phenotypic correlations with sesame yield on every environment except LP21. On LP20 and NP21, scans 1 and 2 displayed significant phenotypic correlations despite low NDVI values. Genetic correlations between NDVI and the yield were always higher than those of the phenotypic correlations as in the case of NDRE. NDVI correlation values ranged from -0.276 to 0.538 and from -0.420 to 0.660 for r_p and r_g , respectively. Negative correlations observed for both SRIs at the beginning of both planting dates and years (first and last scans) (Table 6). SPAD significantly varied between genotypes only on NP20 and LP20 and exhibited negative, and in some cases significant, phenotypic and genotypic correlations with sesame yield for both planting dates and years (Table 6).

3.4. Heritability and Efficiency of Indirect Selection

A moderate to high level of broad-sense heritability was observed for most vegetation indices as values ranged from 0.292 to 0.879 and from 0.446 to 0.928 for NDRE and NDVI, respectively. The heritability of spectral reflectance indices generally increased with the growth stage for a given planting date and year and started to reduce entering the ripening stage of sesame. The highest heritability was found for NDVI at LP20, where it began at 0.446 on the first monitoring date (NDVI1), peaked at 0.928 at NDVI5 and at NDVI7 fell to 0.716 . NDVI showed higher heritability than NDRE in every case except NP20 (Table 6). For SPAD, heritability ranged from 0.095 to 0.698 . Sesame yield showed significant variance between genotypes across all growing conditions and cropping years and high level of heritability with a range from 0.847 to 0.963 (Table 6). The predicted efficiency (E_r) of an indirect SRI-based selection relative to direct selection for sesame yield was in the range of -45 to 61% and -34 to 57% for NDRE and NDVI, respectively. The SRIs from scans 4, 5 and 6 gave the greatest possible interest for indirect selection in relation to direct selection for yield. A total of 61% of the direct selection was the maximum value for NDRE5.

3.5. Adaptive Response of SRIs

The exploitation of adaptive traits as selection criteria requires high broad-sense heritability over environments as a result of high genetic variation and low genotype with environment (GE) interaction and experiment error [65]. All the SRIs displayed significant genotypic effect and GE interaction. Possible interest in breeding for wide adaptation was given by the indices that had moderate to high heritability as indicated by at least 20% of the variation among plots due to genetic effects and at least 70% among lines ($H_x^2 > 0.20$, $H_y^2 > 0.70$, Table 4). NDRE4, NDRE6, NDVI1, NDVI3, NDVI5 and NDVI7 gave high heritability values and among them only NDRE6, NDVI1 and NDVI7 combined with relatively low GE interaction. Yield had the highest heritability values but the largest GE interaction, while SPAD also displayed low adaptive response (Table 7).

3.6. Cluster Analysis

For the agglomerative hierarchical clustering, the Euclidean distance was used as metric and the unweighted average as linkage criterion (UPGMA), to group the genotypes into clusters of increasing dissimilarity based on selected vegetation indices (NDRE5, NDVI4, NDVI5, NDVI6). The dendrogram of Figure 7 shows the 24 sesame lines and landraces split into three groups. Group 1 (displayed in the blue color) contained 7 genotypes, group 2 (displayed in the orange color) had 8 genotypes and group 3 (displayed in the grey color)

included 9 genotypes. Cluster 1 includes mostly the original landraces and the very early maturing lines, clusters 2 and 3 include the mid and late maturing lines, respectively.

Table 7. *p*-Values for Likelihood Ratio Test of the analyzed SRIs for genotype and genotype-vs-environment random effects, broad-sense heritability on a plot basis over environments (H^2_x), and broad-sense heritability on an entry mean basis over the test environments (H^2_y).

SRI	GEN		GEN:ENV		H^2_x	H^2_y	SRI	GEN		GEN:ENV		H^2_x	H^2_y
NDRE1	0.00335	***	0.00947	***	0.119	0.608	NDVI1	0.02254	**	0.00116	***	0.093	0.521
NDRE2	0.015	**	0.00039	***	0.103	0.543	NDVI2	1.31×10^{-9}	**	1.31×10^{-2}	**	0.323	0.847
NDRE3	2.80×10^{-3}	***	1.83×10^{-8}	***	0.158	0.614	NDVI3	1.17×10^{-6}	***	3.50×10^{-7}	***	0.285	0.780
NDRE4	8.16×10^{-5}	***	6.31×10^{-6}	***	0.207	0.711	NDVI4	4.72×10^{-4}	***	1.44×10^{-10}	***	0.203	0.669
NDRE5	1.29×10^{-8}	***	1.35×10^{-6}	***	0.347	0.829	NDVI5	2.71×10^{-6}	***	4.13×10^{-14}	***	0.313	0.769
NDRE6	3.32×10^{-5}	***	5.13×10^{-3}	***	0.193	0.728	NDVI6	3.48×10^{-7}	***	6.31×10^{-8}	***	0.310	0.795
NDRE7	0.29578	***	0.00012	***	0.040	0.293	NDVI7	2.93×10^{-6}	***	2.30×10^{-3}	***	0.233	0.768
NDRE8	1.64×10^{-5}	***	5.96×10^{-4}	***	0.215	0.741	NDVI8	2.87×10^{-10}	***	3.12×10^{-2}	**	0.333	0.858
SPAD	1.16×10^{-6}	***	1.00	NS	0.168	0.764	YIELD	6.16×10^{-8}	***	4.38×10^{-22}	***	0.407	0.814

GEN—Effect of the genotype to the SRIs, SPAD and Yield variance over the test environments. GEN:ENV—Effect of the genotype with environment interaction to the SRIs, SPAD and Yield variance over the test environments. ** = $p < 0.05$, *** = $p < 0.01$.

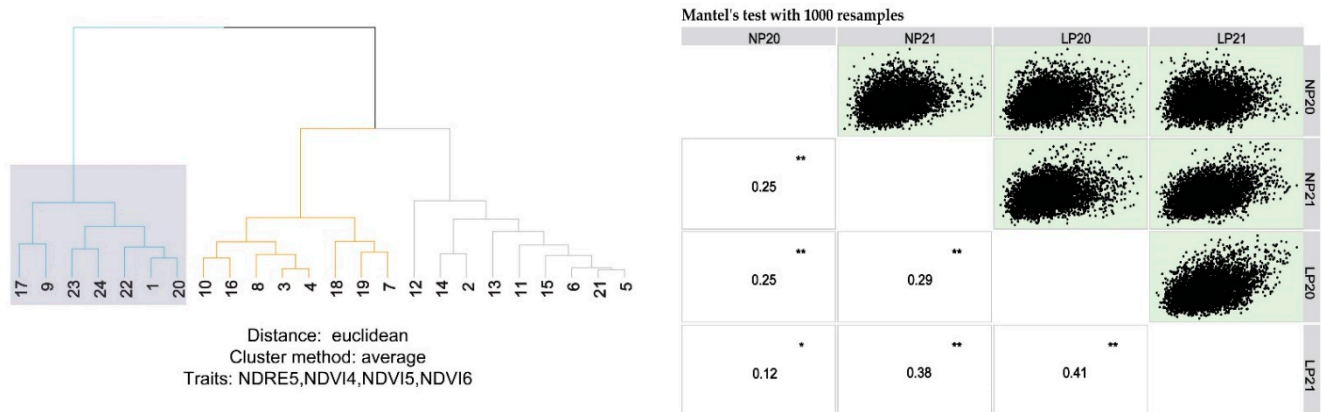


Figure 7. Dendrogram of the agglomerative hierarchical clustering for the 24 sesame genotypes based on selected vegetation indices (NDRE5, NDVI4, NDVI5, NDVI6) (left). Mantel’s test correlation values among planting dates and years (right). * = $p < 0.05$, ** = $p < 0.01$.

To check the relationships between the distance matrices when the clustering is performed separately for each growing condition and cropping year (NP20, LP20, NP21, LP21) a Mantel’s test was performed. The values of correlation between the distance matrices (0.12 to 0.41) suggest that clustering genotypes based on SRI indices, should not vary significantly among planting dates and years (Figure 7).

4. Discussion

The SRI values of 24 sesame lines and landraces were estimated in this study for the first time using active canopy sensors over the entire growing period and in two different planting dates. Previously, only Dong et al. 2020, in experiments in Texas (USA) [51], demonstrated ground-based sensing tool usefulness of vegetation indices for characterizing the dry down process of sesame.

The active canopy sensor used in this study distinguished the different genotypes in almost every reflectance monitoring date suggesting that canopy sensors can be used in sesame breeding programs. All the scans produced SRIs with significant variation among genotypes and significant GE interaction.

Both NDVI and NDRE reached about the same accuracy in genotype phenotyping, even under dense biomass conditions (2–5 scans) where “saturation” problems were expected especially for NDVI as has been reported by many researchers for other crops [65–67].

At those dense biomass conditions, NDVI demonstrated efficient separation between genotypes probably due to the Crop Circle canopy sensors high properties [42,68]. NDRE however acted more precisely in depicting variations among different scan days in regard to NDVI. NDRE produced values (mean from every genotype) at the closed canopy period with differences between consecutive scans up to 13% in regard to 3% differences with NDVI. Therefore, in this study the combination of both indices produced the most accurate sesame phenotyping as suggested by Boiarski et al. [69].

Generally, genotypic and phenotypic correlations among traits of crop plants are useful in planning, evaluating and setting selection criteria for the desired traits for selection in a breeding program. The genetic correlation between traits describes the intrinsic consistency of genotype response across growing conditions and contributes crucially to assess the predicted efficiency of different phenotypic selection strategies [70]. The precise estimation of this inherent association requires a genetically diverse population that accounts for sampling error bias in gene frequency [71]. In our experiment, the 5 landraces and 18 sesame lines derived by them, met the above criterion. Both SRIs significantly correlated with the yield at different monitoring dates throughout growing conditions and cropping years. The highest correlation demonstrated by scans at the end of the sesame reproductive stage and at the beginning of the ripening stage, suggesting the possibility of using these proxy measurements to understand the genetic and physiological basis of yield formation. Overall, these results agree with the findings presented by Dong et al. [51] where working with 60 sesame genotypes reported that NDVI values during the initial nine days after the end of the ripening stage had a significant relationship with the measured seed yields. However, more research is needed to understand the correlation with yield in the beginning of the ripening stage, when chlorophyll degradation occurs.

At both planting dates and years, genetic correlation coefficients were found to be higher in magnitude than that of phenotypic correlation coefficients in most of the traits, which clearly indicated the presence of inherent association among SRIs and yield. The moderate to strong genetic correlation of SRIs to sesame yield in the late planting conditions indicates the potential use of an indirect selection approach to identify high yielding and stress tolerant genotypes.

The results of this study showed that higher H^2 values of vegetation indices were obtained at the end of the reproductive stage and the beginning of the ripening stage. Particularly NDRE5, NDVI5, NDVI6 in 2020 late planting (LP20) displayed values even higher than the yield's heritability.

Broad sense heritability (H^2) is a parameter that expresses the proportion of the phenotypic variance that can be attributed to variance of all genotypic effects, additivity, dominance and epistasis [72,73]. Despite continuous misunderstandings and controversies over its use and application, heritability remains a key issue to the response to selection. Recent reports of substantial heritability for gene expression and new estimation methods using marker data highlight the relevance of heritability in the genomics era [74]. High heritability and strong phenotypic and genetic correlations between indirect traits and the grain yield are desirable. For the accurate estimation of the relative efficiency (Er) of an alternative indirect selection trait versus direct selection for yield as Falconer proposed and many researchers have followed before [31,65,74–76], both the genetic correlation between the trait and yield and their heritability values are needed. NDVI5 in LP20 had H^2 0.928, higher than the H^2 value of yield that was 0.847, but the low rg (0.359) between them resulted to 60% less Er for indirect selection. A similar Er value is given by NDRE6 in NP20 with a very low heritability (0.292) and a high rg (0.748). The highest Er value for indirect SRI-based selection, reached 60% in comparison to direct selection for yield. Indirect SRI-based selection produced better results in normal planting for both years when phenotyping was applied at the end of the sesame reproductive stage.

Heritability over the test environments both on a plot basis and on a line mean basis was moderate to high almost for all the phenotyping dates ($H^2_x > 0.20$, $H^2_y > 0.70$, respectively) for both SRIs, NDVI though demonstrated higher values than NDRE. Nevertheless,

SRI's adaptive response was moderate due to their significantly high effect of the genotype with environment interaction. Research in more environments is needed to identify SRI's value for wide adaptation breeding programs.

Cluster analysis highlighted the importance of identifying the monitoring dates for accurate and functional phenotyping. NDVI and NDRE values at the end of growing and the beginning of ripening stages separated the examined genotypes and produced clusters according to their crop growing cycle length. The analysis produced 3 clusters from which the first consists of the short growth cycle genotypes and furthermore it contains the four lowest yielding genotypes. Clusters 2 and 3 contain the medium and late growth cycle genotypes, respectively, clearly suggesting that the spectral reflectance indices could be a functional, economical and easy to use tool for classifying cultivars into groups.

SPAD showed a non-significant distinguishing ability between sesame genotypes in some environments, negative weak or significant correlations with yield and low to moderate heritability. SPAD was the only trait with non-significant GE interaction. The findings of the present study confirmed the superiority of SRI's compared to SPAD measurements as predictors of yield, which is in accordance with similar studies in wheat [77], but more measures in different stages of the growing period are needed to clarify its contribution to a sesame breeding program.

5. Conclusions

Designing an efficient breeding strategy for improving traits of interest, requires knowledge of quantitative genetic parameters (i.e., variances, heritability, correlated response of traits) and the stability of these parameters across target environments and different genetic backgrounds.

This field study demonstrated the significance of using a ground-based remote sensing tool, such as the simple backpack sensing frame equipped with a Crop Circle sensor, for sesame phenotyping. Both NDVI and NDRE can be used to depict sesame development accurately over the growing season. It was elucidated that in order to use them for accurate genotype differentiation, it is required firstly to identify the monitoring dates with the best phenotyping precision.

Integrating the easily and economically measured spectral reflectance indices in a sesame breeding program can alleviate the costs entailed by a direct selection for yield, a multi-environment selection and the difficulty of applying both of them to early selection stages.

For future research, spectral reflectance in sesame breeding should be studied, not just as a standalone indirect selection criterion, but also as a component in an integrated selection approach. More frequent monitoring of the vegetation indices during the important time window that encompasses the late flowering and the beginning of the ripening stage is recommended to capture detailed changes in sesame canopy features. In addition, combining data from different monitoring days to create a complex SRI index could improve genotype classification and genetic correlation with yield.

Author Contributions: Conceptualization, C.P., E.E. and D.N.V.; methodology, C.P., E.E. and D.N.V.; validation, C.P., E.E. and D.N.V.; formal analysis, C.P., E.E. and D.N.V.; investigation, C.P., E.E. and A.K.; resources, C.P., E.E. and D.N.V.; data curation, C.P., E.E., A.T. and A.K.; writing—original draft preparation, C.P.; writing—review and editing, C.P., E.E., V.A., O.I.P., E.K. and D.N.V.; visualization, C.P. and A.T.; supervision, D.N.V. All authors have read and agreed to the published version of the manuscript.

Funding: This research received no external funding.

Data Availability Statement: The data presented in this study are available on request from the corresponding author. The data are not publicly available due to privacy restrictions.

Acknowledgments: The study was part of the Ph.D. thesis “Genetic improvement of sesame landraces and evaluation of superior lines using high-throughput phenotyping” supervised by the Laboratory of Genetics and Plant Breeding of University of Thessaly and supported by the Institute of Industrial and Forage Crops of Hellenic Agricultural Organization. We thank the staff of the Institute of Industrial and Forage Crops for their help during the course of experimentation.

Conflicts of Interest: The authors declare no conflict of interest.

References

1. Bedigian, D.; Harlan, J.R. Evidence for Cultivation of Sesame in the Ancient World. *Econ. Bot.* **1986**, *40*, 137–154. [[CrossRef](#)]
2. Bedigian, D. Characterization of Sesame (*Sesamum indicum* L.) Germplasm: A Critique. *Genet. Resour. Crop Evol.* **2010**, *57*, 641–647. [[CrossRef](#)]
3. Douché, C.; Tsirtsis, K.; Margaritis, E. What's New during the First Millennium BCE in Greece? Archaeobotanical Results from Olynthos and Sikyon. *J. Archaeol. Sci. Rep.* **2021**, *36*, 102782. [[CrossRef](#)]
4. Food and Agriculture Organization Statistical Databases (FAOSTAT). FAOSTAT Provides Free Access to Food and Agriculture Data for Over 245 Countries and Territories and Covers All FAO Regional Groupings. Available online: <http://faostat.fao.org/> (accessed on 15 December 2021).
5. Anilakumar, K.R.; Pal, A.; Khanum, F.; Bawa, A.S. Nutritional, medicinal and industrial uses of sesame (*Sesamum indicum* L.) seeds—An overview. *Agric. Consp. Sci.* **2010**, *75*, 159–168.
6. Namiki, M. Nutraceutical Functions of Sesame: A Review. *Crit. Rev. Food Sci. Nutr.* **2007**, *47*, 651–673. [[CrossRef](#)]
7. da Silva Barbosa, C.V.; Silva, A.S.; de Oliveira, C.V.C.; Massa, N.M.L.; de Sousa, Y.R.F.; da Costa, W.K.A.; Silva, A.C.; Delatorre, P.; Carvalho, R.; Braga, V.; et al. Effects of Sesame (*Sesamum indicum* L.) Supplementation on Creatine Kinase, Lactate Dehydrogenase, Oxidative Stress Markers, and Aerobic Capacity in Semi-Professional Soccer Players. *Front. Physiol.* **2017**, *8*, 196. [[CrossRef](#)]
8. Cheng, F.-C.; Jinn, T.-R.; Hou, R.C.W.; Tzen, J.T.C. Neuroprotective Effects of Sesamin and Sesamol on Gerbil Brain in Cerebral Ischemia. *Int. J. Biomed. Sci.* **2006**, *2*, 284–288.
9. Gloaguen, R.M.; Byrd, S.; Rowland, D.L.; Langham, D.R.; Couch, A. Planting Date and Row Spacing Effects on the Agronomic Potential of Sesame in the Southeastern USA. *J. Crop Improv.* **2018**, *32*, 387–417. [[CrossRef](#)]
10. Couch, A.; Gloaguen, R.M.; Langham, D.R.; Hochmuth, G.J.; Bennett, J.M.; Rowland, D.L. Non-Dehiscent Sesame (*Sesamum indicum* L.): Its Unique Production Potential and Expansion into the Southeastern USA. *J. Crop Improv.* **2017**, *31*, 101–172. [[CrossRef](#)]
11. Gloaguen, R.M.; Couch, A.; Rowland, D.L.; Bennett, J.; Hochmuth, G.; Langham, D.R.; Brym, Z.T. Root Life History of Non-Dehiscent Sesame (*Sesamum indicum* L.) Cultivars and the Relationship with Canopy Development. *Field Crops Res.* **2019**, *241*, 107560. [[CrossRef](#)]
12. Islam, F.; Gill, R.A.; Ali, B.; Farooq, M.A.; Xu, L.; Najeeb, U.; Zhou, W. Chapter 6-Sesame. In *Breeding Oilseed Crops for Sustainable Production*; Gupta, S.K., Ed.; Academic Press: San Diego, CA, USA, 2016; pp. 135–147. [[CrossRef](#)]
13. Langham, D.R.; Weimers, T. Progress in Mechanizing Sesame in the US through Breeding. In *Trends in New Crops and New Uses*; Janick, J., Whipkey, A., Eds.; ASHS Press: Alexandria, VA, USA, 2002; pp. 157–173.
14. Dossa, K.; Diouf, D.; Wang, L.; Wei, X.; Zhang, Y.; Niang, M.; Fonceka, D.; Yu, J.; Mmadi, M.A.; Yehouessi, L.W.; et al. The Emerging Oilseed Crop *Sesamum indicum* Enters the “Omics” Era. *Front. Plant Sci.* **2017**, *8*, 1154. [[CrossRef](#)] [[PubMed](#)]
15. Cui, C.; Liu, Y.; Liu, Y.; Cui, X.; Sun, Z.; Du, Z.; Wu, K.; Jiang, X.; Mei, H.; Zheng, Y. Genome-Wide Association Study of Seed Coat Color in Sesame (*Sesamum indicum* L.). *PLoS ONE* **2021**, *16*, e0251526. [[CrossRef](#)] [[PubMed](#)]
16. Wei, X.; Gong, H.; Yu, J.; Liu, P.; Wang, L.; Zhang, Y.; Zhang, X. SesameFG: An Integrated Database for the Functional Genomics of Sesame. *Sci. Rep.* **2017**, *7*, 2342. [[CrossRef](#)]
17. Awada, L.; Phillips, P.W.B.; Smyth, S.J. The Adoption of Automated Phenotyping by Plant Breeders. *Euphytica* **2018**, *214*, 148. [[CrossRef](#)]
18. Singh, B.D.; Singh, A.K. Phenomics. In *Marker-Assisted Plant Breeding: Principles and Practices*; Singh, B.D., Singh, A.K., Eds.; Springer: New Delhi, India, 2015; pp. 431–461. [[CrossRef](#)]
19. Kumar, J.; Pratap, A.; Kumar, S. *Phenomics in Crop Plants: Trends, Options and Limitations*; Springer: New Delhi, India, 2015.
20. Mir, R.R.; Reynolds, M.; Pinto, F.; Khan, M.A.; Bhat, M.A. High-Throughput Phenotyping for Crop Improvement in the Genomics Era. *Plant Sci.* **2019**, *282*, 60–72. [[CrossRef](#)]
21. Jung, J.; Maeda, M.; Chang, A.; Bhandari, M.; Ashapure, A.; Landivar-Bowles, J. The Potential of Remote Sensing and Artificial Intelligence as Tools to Improve the Resilience of Agriculture Production Systems. *Curr. Opin. Biotechnol.* **2021**, *70*, 15–22. [[CrossRef](#)]
22. Watson, A.; Ghosh, S.; Williams, M.J.; Cuddy, W.S.; Simmonds, J.; Rey, M.-D.; Asyraf Md Hatta, M.; Hinchliffe, A.; Steed, A.; Reynolds, D.; et al. Speed Breeding Is a Powerful Tool to Accelerate Crop Research and Breeding. *Nat. Plants* **2018**, *4*, 23–29. [[CrossRef](#)]
23. Araus, J.L.; Kefauver, S.C.; Zaman-Allah, M.; Olsen, M.S.; Cairns, J.E. Phenotyping: New Crop Breeding Frontier. In *Encyclopedia of Sustainability Science and Technology*; Meyers, R.A., Ed.; Springer: New York, NY, USA, 2018; pp. 1–11. [[CrossRef](#)]
24. Duan, T.; Chapman, S.C.; Guo, Y.; Zheng, B. Dynamic Monitoring of NDVI in Wheat Agronomy and Breeding Trials Using an Unmanned Aerial Vehicle. *Field Crops Res.* **2017**, *210*, 71–80. [[CrossRef](#)]
25. Brown, M.; de Beurs, K. Evaluation of Multi-Sensor Semi-Arid Crop Season Parameters Based on NDVI and Rainfall. *Remote Sens. Environ.* **2008**, *112*, 2261–2271. [[CrossRef](#)]
26. Erdle, K.; Mistele, B.; Schmidhalter, U. Comparison of Active and Passive Spectral Sensors in Discriminating Biomass Parameters and Nitrogen Status in Wheat Cultivars. *Field Crops Res.* **2011**, *124*, 74–84. [[CrossRef](#)]
27. Huang, J.; Wang, H.; Dai, Q.; Han, D. Analysis of NDVI Data for Crop Identification and Yield Estimation. *IEEE J. Sel. Top. Appl. Earth Obs. Remote Sens.* **2014**, *7*, 4374–4384. [[CrossRef](#)]

28. Cabrera-Bosquet, L.; Molero, G.; Stellacci, A.; Bort, J.; Nogués, S.; Araus, J. NDVI as a Potential Tool for Predicting Biomass, Plant Nitrogen Content and Growth in Wheat Genotypes Subjected to Different Water and Nitrogen Conditions. *Cereal Res. Commun.* **2011**, *39*, 147–159. [[CrossRef](#)]
29. Kyrtzizis, A.; Skarlatos, D.; Fotopoulos, V.; Vamvakousis, V.; Katsiotis, A. Investigating Correlation among NDVI Index Derived by Unmanned Aerial Vehicle Photography and Grain Yield under Late Drought Stress Conditions. *Procedia Environ. Sci.* **2015**, *29*, 225–226. [[CrossRef](#)]
30. Carter, G.A. Reflectance Wavebands and Indices for Remote Estimation of Photosynthesis and Stomatal Conductance in Pine Canopies. *Remote Sens. Environ.* **1998**, *63*, 61–72. [[CrossRef](#)]
31. Babar, M.A.; Reynolds, M.P.; van Ginkel, M.; Klatt, A.R.; Raun, W.R.; Stone, M.L. Spectral Reflectance Indices as a Potential Indirect Selection Criteria for Wheat Yield under Irrigation. *Crop Sci.* **2006**, *46*, 578–588. [[CrossRef](#)]
32. Ma, B.L.; Dwyer, L.M.; Costa, C.; Cober, E.R.; Morrison, M.J. Early Prediction of Soybean Yield from Canopy Reflectance Measurements. *Agron. J.* **2001**, *93*, 1227–1234. [[CrossRef](#)]
33. Holland, K.H.; Lamb, D.W.; Schepers, J.S. Radiometry of Proximal Active Optical Sensors (AOS) for Agricultural Sensing. *IEEE J. Sel. Top. Appl. Earth Obs. Remote Sens.* **2012**, *5*, 1793–1802. [[CrossRef](#)]
34. Holland, K.H.; Schepers, J.S. Use of a Virtual-Reference Concept to Interpret Active Crop Canopy Sensor Data. *Precis. Agric.* **2013**, *14*, 71–85. [[CrossRef](#)]
35. Shaver, T.M.; Khosla, R.; Westfall, D.G. Evaluation of Two Crop Canopy Sensors for Nitrogen Variability Determination in Irrigated Maize. *Precis. Agric.* **2011**, *12*, 892–904. [[CrossRef](#)]
36. Holland Scientific. *Crop Circle ACS-430 Users' Guide*; Holland Scientific: Lincoln, NE, USA, 2010; Available online: www.hollandscientific.com (accessed on 5 March 2022).
37. Holland, K.H.; Schepers, J.S. Derivation of a Variable Rate Nitrogen Application Model for In-Season Fertilization of Corn. *Agron. J.* **2010**, *102*, 1415–1424. [[CrossRef](#)]
38. Sharma, L.K.; Bu, H.; Denton, A.; Franzen, D.W. Active-Optical Sensors Using Red NDVI Compared to Red Edge NDVI for Prediction of Corn Grain Yield in North Dakota, U.S.A. *Sensors* **2015**, *15*, 7832. [[CrossRef](#)] [[PubMed](#)]
39. Aranguren, M.; Castellón, A.; Aizpurua, A. Wheat Yield Estimation with NDVI Values Using a Proximal Sensing Tool. *Remote Sens.* **2020**, *12*, 2749. [[CrossRef](#)]
40. Inman, D.; Khosla, R.; Mayfield, T. On-the-go Active Remote Sensing for Efficient Crop Nitrogen Management. *Sens. Rev.* **2005**, *25*, 209–214. [[CrossRef](#)]
41. Amaral, L.R.; Molin, J.P.; Portz, G.; Finazzi, F.B.; Cortinove, L. Comparison of Crop Canopy Reflectance Sensors Used to Identify Sugarcane Biomass and Nitrogen Status. *Precis. Agric.* **2015**, *16*, 15–28. [[CrossRef](#)]
42. Bonfil, D.J. Wheat Phenomics in the Field by RapidScan: NDVI vs. NDRE. *Isr. J. Plant Sci.* **2017**, *64*, 41–54. [[CrossRef](#)]
43. Darra, N.; Psomiadis, E.; Kasimati, A.; Anastasiou, A.; Anastasiou, E.; Fountas, S. Remote and Proximal Sensing-Derived Spectral Indices and Biophysical Variables for Spatial Variation Determination in Vineyards. *Agronomy* **2021**, *11*, 741. [[CrossRef](#)]
44. Krause, M.R.; Mondal, S.; Crossa, J.; Singh, R.P.; Pinto, F.; Haghhighattalab, A.; Shrestha, S.; Rutkoski, J.; Gore, M.A.; Sorrells, M.E.; et al. Aerial High-Throughput Phenotyping Enables Indirect Selection for Grain Yield at the Early Generation, Seed-Limited Stages in Breeding Programs. *Crop Sci.* **2020**, *60*, 3096–3114. [[CrossRef](#)]
45. Rutkoski, J.; Poland, J.; Mondal, S.; Autrique, E.; Pérez, L.G.; Crossa, J.; Reynolds, M.; Singh, R. Canopy Temperature and Vegetation Indices from High-Throughput Phenotyping Improve Accuracy of Pedigree and Genomic Selection for Grain Yield in Wheat. *G3 Genes | Genomes | Genetics* **2016**, *6*, 2799–2808. [[CrossRef](#)]
46. Hu, Y.; Knapp, S.; Schmidhalter, U. Advancing High-Throughput Phenotyping of Wheat in Early Selection Cycles. *Remote Sens.* **2020**, *12*, 574. [[CrossRef](#)]
47. Anderegg, J.; Yu, K.; Aasen, H.; Walter, A.; Liebisch, F.; Hund, A. Spectral Vegetation Indices to Track Senescence Dynamics in Diverse Wheat Germplasm. *Front Plant Sci.* **2020**, *10*, 1749. [[CrossRef](#)]
48. Naser, M.A.; Khosla, R.; Longchamps, L.; Dahal, S. Using NDVI to Differentiate Wheat Genotypes Productivity under Dryland and Irrigated Conditions. *Remote Sens.* **2020**, *12*, 824. [[CrossRef](#)]
49. Lindsey, A.J.; Craft, J.C.; Barker, D.J. Modeling Canopy Senescence to Calculate Soybean Maturity Date Using NDVI. *Crop Sci.* **2020**, *60*, 172–180. [[CrossRef](#)]
50. Christenson, B.S.; Schapaugh, W.T., Jr.; An, N.; Price, K.P.; Prasad, V.; Fritz, A.K. Predicting Soybean Relative Maturity and Seed Yield Using Canopy Reflectance. *Crop Sci.* **2016**, *56*, 625–643. [[CrossRef](#)]
51. Dong, X.; Feng, G.; Zemach, I. Using Normalized Difference Vegetation Index to Estimate Sesame Drydown and Seed Yield. *J. Crop Improv.* **2021**, *35*, 508–521. [[CrossRef](#)]
52. Peel, M.C.; Finlayson, B.L.; McMahon, T.A. Updated World Map of the Köppen-Geiger Climate Classification. *Hydrol. Earth Syst. Sci.* **2007**, *11*, 1633–1644. [[CrossRef](#)]
53. Nachtergaele, F. Soil Taxonomy—a Basic System of Soil Classification for Making and Interpreting Soil Surveys: Second Edition, by Soil Survey Staff, 1999, USDA–NRCS, Agriculture Handbook Number 436, Hardbound. *Geoderma* **2001**, *99*, 336–337. [[CrossRef](#)]
54. Vlachostergios, D.N.; Tzantarmas, C.; Kargiotidou, A.; Ninou, E.; Pankou, C.; Gaintatzi, C.; Mylonas, I.; Papadopoulos, I.; Foti, C.; Chatzivassiliou, E.K.; et al. Single-Plant Selection within Lentil Landraces at Ultra-Low Density: A Short-Time Tool to Breed High Yielding and Stable Varieties across Divergent Environments. *Euphytica* **2018**, *214*, 58. [[CrossRef](#)]

55. Ninou, E.; Papathanasiou, F.; Vlachostergios, D.N.; Mylonas, I.; Kargiotidou, A.; Pankou, C.; Papadopoulos, I.; Sinapidou, E.; Tokatlidis, I. Intense Breeding within Lentil Landraces for High-Yielding Pure Lines Sustained the Seed Quality Characteristics. *Agriculture* **2019**, *9*, 175. [[CrossRef](#)]
56. Fasoula, D.A.; Ioannides, I.M.; Omirou, M. Phenotyping and Plant Breeding: Overcoming the Barriers. *Front. Plant Sci.* **2020**, *10*, 1713. [[CrossRef](#)]
57. Angus, J.F.; Cunningham, R.B.; Moncur, M.W.; Mackenzie, D.H. Phasic Development in Field Crops I. Thermal Response in the Seedling Phase. *Field Crops Res.* **1980**, *3*, 365–378. [[CrossRef](#)]
58. Meena, H.; Rao, A.V.B. Growing Degree Days Requirement of Sesame (*Sesamum Indicum*) in Relation to Growth and Phenological Development in Western Rajasthan. *Curr. Adv. Agric. Sci.* **2013**, *5*, 107–110.
59. R Core Team. *R: A Language and Environment for Statistical Computing*; R Foundation for Statistical Computing: Vienna, Austria, 2021; Available online: <https://www.R-project.org/> (accessed on 7 February 2022).
60. De Mendiburu, F. Una Herramienta de Análisis Estadístico para la Investigación Agrícola. Master's Thesis, Facultad de Economía y Planificación, Departamento Académico de Estadística e Informática, Universidad Nacional de Ingeniería (UNI-PERU), Lima, Peru, 2009.
61. Olivoto, T.; Lúcio, A.D. Metan: An R Package for Multi-Environment Trial Analysis. *Methods Ecol. Evol.* **2020**, *11*, 783–789. [[CrossRef](#)]
62. Falconer, D.S. *Introduction to Quantitative Genetics*, 4th ed.; Prentice Hall: Harlow, UK, 1996.
63. Holland, J.; Nyquist, W.E.; Cervantes-Martinez, C.T. Estimating and Interpreting Heritability for Plant Breeding: An update. *Plant Breed. Rev.* **2003**, *22*, 9–111.
64. Annicchiarico, P.; Iannucci, A. Adaptation Strategy, Germplasm Type and Adaptive Traits for Field Pea Improvement in Italy Based on Variety Responses across Climatically Contrasting Environments. *Field Crops Res.* **2008**, *108*, 133–142. [[CrossRef](#)]
65. Gizaw, S.A.; Garland-Campbell, K.; Carter, A.H. Use of Spectral Reflectance for Indirect Selection of Yield Potential and Stability in Pacific Northwest Winter Wheat. *Field Crops Res.* **2016**, *196*, 199–206. [[CrossRef](#)]
66. Gizaw, S.A.; Garland-Campbell, K.; Carter, A.H. Evaluation of Agronomic Traits and Spectral Reflectance in Pacific Northwest Winter Wheat under Rain-Fed and Irrigated Conditions. *Field Crops Res.* **2016**, *196*, 168–179. [[CrossRef](#)]
67. Moriondo, M.; Maselli, F.; Bindi, M. A Simple Model of Regional Wheat Yield Based on NDVI Data. *Eur. J. Agron.* **2007**, *26*, 266–274. [[CrossRef](#)]
68. Kipp, S.; Mistele, B.; Schmidhalter, U. The Performance of Active Spectral Reflectance Sensors as Influenced by Measuring Distance, Device Temperature and Light Intensity. *Comput. Electron. Agric.* **2014**, *100*, 24–33. [[CrossRef](#)]
69. Boiarskii, B. Comparison of NDVI and NDRE Indices to Detect Differences in Vegetation and Chlorophyll Content. *J. Mech. Contin. Math. Sci. Spl1* **2019**, *4*, 20–29. [[CrossRef](#)]
70. Annicchiarico, P.; Nazzicari, N.; Notario, T.; Monterrubio Martin, C.; Romani, M.; Ferrari, B.; Pecetti, L. Pea Breeding for Intercropping With Cereals: Variation for Competitive Ability and Associated Traits, and Assessment of Phenotypic and Genomic Selection Strategies. *Front Plant Sci.* **2021**, *12*, 731949. [[CrossRef](#)]
71. Bohren, B.B.; McKean, H.E.; Yamada, Y. Relative Efficiencies of Heritability Estimates Based on Regression of Offspring on Parent. *Biometrics* **1961**, *17*, 481–491. [[CrossRef](#)]
72. Schmidt, P.; Hartung, J.; Bennewitz, J.; Piepho, H.-P. Heritability in Plant Breeding on a Genotype-Difference Basis. *Genetics* **2019**, *212*, 991–1008. [[CrossRef](#)] [[PubMed](#)]
73. Visscher, P.M.; Hill, W.G.; Wray, N.R. Heritability in the Genomics Era—Concepts and Misconceptions. *Nat. Rev. Genet.* **2008**, *9*, 255–266. [[CrossRef](#)] [[PubMed](#)]
74. Bowman, B.C.; Chen, J.; Zhang, J.; Wheeler, J.; Wang, Y.; Zhao, W.; Nayak, S.; Heslot, N.; Bockelman, H.; Bonman, J.M. Evaluating Grain Yield in Spring Wheat with Canopy Spectral Reflectance. *Crop Sci.* **2015**, *55*, 1881–1890. [[CrossRef](#)]
75. Gutierrez, M.; Reynolds, M.P.; Raun, W.R.; Stone, M.L.; Klatt, A.R. Spectral Water Indices for Assessing Yield in Elite Bread Wheat Genotypes under Well-Irrigated, Water-Stressed, and High-Temperature Conditions. *Crop Sci.* **2010**, *50*, 197–214. [[CrossRef](#)]
76. Lozada, D.N.; Godoy, J.V.; Ward, B.P.; Carter, A.H. Genomic Prediction and Indirect Selection for Grain Yield in US Pacific Northwest Winter Wheat Using Spectral Reflectance Indices from High-Throughput Phenotyping. *Int. J. Mol. Sci.* **2019**, *21*, 165. [[CrossRef](#)]
77. Kyratzis, A.C.; Skarlatos, D.P.; Menexes, G.C.; Vamvakousis, V.F.; Katsiotis, A. Assessment of Vegetation Indices Derived by UAV Imagery for Durum Wheat Phenotyping under a Water Limited and Heat Stressed Mediterranean Environment. *Front Plant Sci.* **2017**, *8*, 1114. [[CrossRef](#)]